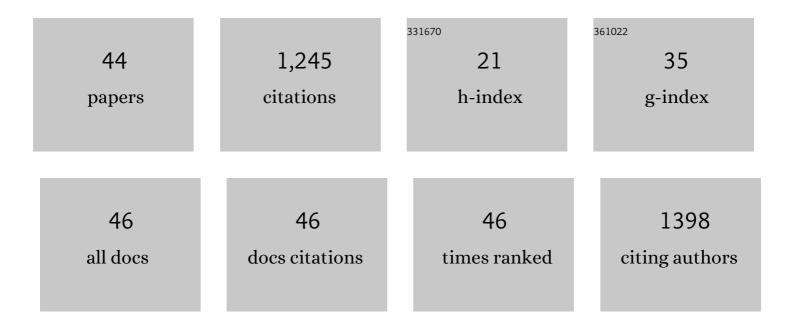
Mario Zarroca

List of Publications by Year in descending order

Source: https://exaly.com/author-pdf/912764/publications.pdf Version: 2024-02-01



#	Article	IF	CITATIONS
1	Tsunami waves extensively resurfaced the shorelines of an early Martian ocean. Scientific Reports, 2016, 6, 25106.	3.3	121
2	Electrical methods (VES and ERT) for identifying, mapping and monitoring different saline domains in a coastal plain region (Alt EmpordA, Northern Spain). Journal of Hydrology, 2011, 409, 407-422.	5.4	103
3	Evaluation of trenching, ground penetrating radar (GPR) and electrical resistivity tomography (ERT) for sinkhole characterization. Earth Surface Processes and Landforms, 2014, 39, 214-227.	2.5	81
4	Investigating gravitational grabens related to lateral spreading and evaporite dissolution subsidence by means of detailed mapping, trenching, and electrical resistivity tomography (Spanish Pyrenees). Lithosphere, 2012, 4, 331-353.	1.4	68
5	Sinkhole investigation in an urban area by trenching in combination with GPR, ERT and high-precision leveling. Mantled evaporite karst of Zaragoza city, NE Spain. Engineering Geology, 2017, 231, 9-20.	6.3	59
6	Differentiating between gravitational and tectonic faults by means of geomorphological mapping, trenching and geophysical surveys. The case of the Zenzano Fault (Iberian Chain, N Spain). Geomorphology, 2013, 189, 93-108.	2.6	53
7	Investigating a damaging buried sinkhole cluster in an urban area (Zaragoza city, NE Spain) integrating multiple techniques: Geomorphological surveys, DInSAR, DEMs, GPR, ERT, and trenching. Geomorphology, 2015, 229, 3-16.	2.6	53
8	Quantifying groundwater discharge from different sources into a Mediterranean wetland by using 222Rn and Ra isotopes. Journal of Hydrology, 2012, 466-467, 11-22.	5.4	48
9	Late Holocene episodic displacement on fault scarps related to interstratal dissolution of evaporites (Teruel Neogene Graben, NE Spain). Journal of Structural Geology, 2012, 34, 2-19.	2.3	46
10	Large landslides associated with a diapiric fold in Canelles Reservoir (Spanish Pyrenees): Detailed geological–geomorphological mapping, trenching and electrical resistivity imaging. Geomorphology, 2015, 241, 224-242.	2.6	46
11	Integrated geophysics and soil gas profiles as a tool to characterize active faults: the Amer fault example (Pyrenees, NE Spain). Environmental Earth Sciences, 2012, 67, 889-910.	2.7	44
12	Application of electrical resistivity imaging (ERI) to a tailings dam project for artisanal and small-scale gold mining in Zaruma-Portovelo, Ecuador. Journal of Applied Geophysics, 2015, 113, 103-113.	2.1	40
13	The impact of droughts and climate change on sinkhole occurrence. A case study from the evaporite karst of the Fluvia Valley, NE Spain. Science of the Total Environment, 2017, 579, 345-358.	8.0	37
14	Characterization of radon levels in soil and groundwater in the North Maladeta Fault area (Central) Tj ETQqO 0 0 Environmental Radioactivity, 2018, 189, 1-13.	rgBT /Ove 1.7	rlock 10 Tf 50 33
15	Soil radon dynamics in the Amer fault zone: An example of very high seasonal variations. Journal of Environmental Radioactivity, 2016, 151, 293-303.	1.7	30
16	Martian outflow channels: How did their source aquifers form and why did they drain so rapidly?. Scientific Reports, 2015, 5, 13404.	3.3	29
17	Sinkholes and caves related to evaporite dissolution in a stratigraphically and structurally complex setting, Fluvia Valley, eastern Spanish Pyrenees. Geological, geomorphological and environmental implications. Geomorphology, 2016, 267, 76-97.	2.6	29
18	Identifying the boundaries of sinkholes and subsidence areas via trenching and establishing setback distances. Engineering Geology, 2018, 233, 255-268.	6.3	27

MARIO ZARROCA

#	Article	IF	CITATIONS
19	Reconstructing the internal structure and long-term evolution of hazardous sinkholes combining trenching, electrical resistivity imaging (ERI) and ground penetrating radar (GPR). Geomorphology, 2017, 285, 287-304.	2.6	26
20	Integrated geophysical and morphostratigraphic approach to investigate a coseismic (?) translational slide responsible for the destruction of the MontclA®s village (Spanish Pyrenees). Landslides, 2014, 11, 655-671.	5.4	24
21	Late Holocene evolution of playa lakes in the central Ebro depression based on geophysical surveys and morpho-stratigraphic analysis of lacustrine terraces. Geomorphology, 2013, 196, 177-197.	2.6	23
22	The application of GPR and ERI in combination with exposure logging and retrodeformation analysis to characterize sinkholes and reconstruct their impact on fluvial sedimentation. Earth Surface Processes and Landforms, 2017, 42, 1049-1064.	2.5	21
23	Delineating coastal groundwater discharge processes in a wetland area by means of electrical resistivity imaging, ²²⁴ Ra and ²²² Rn. Hydrological Processes, 2014, 28, 2382-2395.	2.6	19
24	Subsurface initiation of tafoni in granite terrains — Geophysical evidence from NE Spain: Geomorphological implications. Geomorphology, 2013, 196, 94-105.	2.6	18
25	An assessment of the influence of sulfidic mine wastes on rainwater quality in a semiarid climate (SE) Tj ETQq1	l 0.78431 4.1	4 rgBT /Over
26	Groundwater flow induced collapse and flooding in Noctis Labyrinthus, Mars. Planetary and Space Science, 2016, 124, 1-14.	1.7	18
27	Time-lapse resistivity analysis of Quaternary sediments in the Midlands of Ireland. Journal of Applied Geophysics, 2012, 82, 46-58.	2.1	16
28	Sinkholes in hypogene versus epigene karst systems, illustrated with the hypogene gypsum karst of the Sant Miquel de Campmajor Valley, NE Spain. Geomorphology, 2019, 328, 57-78.	2.6	15
29	Morpho-stratigraphic characterization of a tufa mound complex in the Spanish Pyrenees using ground penetrating radar and trenching, implications for studies in Mars. Earth and Planetary Science Letters, 2014, 388, 197-210.	4.4	12
30	Sedimentological and palaeohydrological characterization of Late Pleistocene and Holocene tufa mound palaeolakes using trenching methods in the Spanish Pyrenees. Sedimentology, 2016, 63, 1786-1819.	3.1	12
31	Paleoflood records from sinkholes using an example from the Ebro River floodplain, northeastern Spain. Quaternary Research, 2017, 88, 71-88.	1.7	10
32	Chronology and paleoenvironmental interpretation of talus flatiron sequences in a subâ€humid mountainous area: Tremp Depression, Spanish Pyrenees. Earth Surface Processes and Landforms, 2013, 38, 1513-1522.	2.5	9
33	The 1997 Mars Pathfinder Spacecraft Landing Site: Spillover Deposits from an Early Mars Inland Sea. Scientific Reports, 2019, 9, 4045.	3.3	9
34	Natural acid rock drainage in alpine catchments: A side effect of climate warming. Science of the Total Environment, 2021, 778, 146070.	8.0	9
35	Origin and evolution of Sariñena Lake (central Ebro Basin): A piping-based model. Geomorphology, 2017, 290, 164-183.	2.6	8
36	Subsidence mechanisms and sedimentation in alluvial sinkholes inferred from trenching and ground penetrating radar (GPR). Implications for subsidence and flooding hazard assessment. Quaternary International, 2019, 525, 1-15.	1.5	7

MARIO ZARROCA

#	Article	IF	CITATIONS
37	Neotectonics and late Holocene paleoseismic evidence in the Plio-Quaternary Daroca Half-graben, Iberian Chain, NE Spain. Implications for fault source characterization. Journal of Structural Geology, 2020, 131, 103933.	2.3	7
38	Granite caves in the north-east of the Iberian Peninsula: Artificial hypogea versus tafoni. Zeitschrift Für Geomorphologie, 2011, 55, 341-364.	0.8	5
39	The Chaotic Terrains of Mercury Reveal a History of Planetary Volatile Retention and Loss in the Innermost Solar System. Scientific Reports, 2020, 10, 4737.	3.3	5
40	North polar trough formation due to in-situ erosion as a source of young ice in mid-latitudinal mantles on Mars. Scientific Reports, 2021, 11, 6750.	3.3	3
41	The episodic rise, net growing rate and kinematics of radial faults of the Salinas de Oro diapir using paleoseismological techniques (NE Spain). Salt upwelling versus karstic subsidence. Geomorphology, 2019, 342, 210-222.	2.6	2
42	Reply to the discussion by Pinyol et al. (2016) on Gutiérrez et al. (2015) "Large landslides associated with a diapiric fold in Canelles Reservoir (Spanish Pyrenees): Detailed geological–geomorphological mapping, trenching and electrical resistivity imaging― Geomorphology, 2016, 263, 175-178.	2.6	0
43	Weathering evolution in lutites of the K/Pg transition red beds of the Tremp Group (Tremp-Isona Basin,) Tj ETQq1	1.0.7843 0.6	14 rgBT /Ov

The Olot Volcanic Field. World Geomorphological Landscapes, 2014, , 249-256.

0.3 0